Journal of
Computational and Theoretical Nanoscience
Vol. 12, 3363–3369, 2015

RESEARCH ARTICLE

3D Molecular Dynamics/Finite Element Simulation of Carbon Nanotubes-Reinforced Polymer Composites

Jaime Horta[1], Witold Brostow[2], Ricardo Simoes[3], and Victor M. Castaño[4,*]

[1] *Facultad de Ingenieria, Universidad Autonoma de Querétaro, Queretaro, 76010, México*
[2] *Laboratory of Advanced Polymers and Optimized Materials, University of North Texas, Denton, 76207, Texas*
[3] *University of Minho, Porto, 4800-019, Portugal*
[4] *Centro de Fisica Aplicada y Tecnologia Avanzada, Universidad Nacional Autonoma de Mexico, Juriquilla, Queretaro, 76230, Mexico*

A simulation of the mechanical behavior of a carnon nanotubes-reinforced polymeric composite, based on Flory's statistical segment approach, is presented. The material is modeled at the micro and nano levels. Interactions between molecules are Morse-like potentials, as well as Van der Walls forces. Traditional simulations involve Molecular Dynamics by solving Newton's equations of motion, Instead, we apply here a finite element approach, involving nonlinear elements to take into account the potential interactions. Amorphous polymer chains are represented by statistical segments, in which several repeating units of a chain are treated as single and independent components. This model allows the simulation at a large scale as compared to those using the unit-atom model or those performed at the atomistic level.

Keywords: Nanotechnology, Carbon Nanotube, Computer Modeling, Bond Stiffness, Non Lineal Analysis.

1. BACKGROUND

Ajayan et al.[1] reported the first polymer nanocomposites using carbon Nanotubes (CNTs) as fillers; since then, CNTs have been used as reinforcements in many high performance polymer composites.[2] The nanocomposites properties depend on the aspect ratio, diameter, and chirality of the nanotubes, as well as on the concentration and dispersion in the matrix. The properties of polymer composites that may improve due to the inclusion of CNTs include tensile strength, tensile modulus, toughness, and electrical and thermal conductivity.[3,4]

The CNTs usually form stable bundles, due to Van der Waals interactions, becoming extremely difficult to disperse and align within a polymer matrix. Despite the considerable advances in the field of CNTs over the past two decades, very little is understood regarding the behavior of polymer nanocomposites, particularly in terms of how exactly the reinforcement effect is achieved, the mechanisms that allow improved dispersion and distribution of the CNTs in the matrix, and how to tailor the properties of the nanocomposites for specific applications.

By using traditional Molecular Dynamics with Newton's equations of motion describing the motion of atoms, the mechanical and thermodynamic properties of the CNTs and the resulting nanocomposites can be studied,[5,6] both at the nano-scale. However, a serious problem that arises, due to the disparities between simulation methods working at different scales, is how to couple them since, between the atomic (discrete) and the continuum scales, there is a bridging zone.[7,8] Another treatment used, the HAC model (Hybrid Atom-continuum), was presented by Wang[9] to calculate the energy of the representative unit cell of hexagonal phases and shape for carbon-carbon bonds. The intratube energy is the bending energy of the wall, while the intertube van der Waals interaction is modeled through a Lennard-Jones potential.

Other solution implies the use of mechanical structural models, at nano and micro-scales. The first case was reported, among others, by Belitchko,[10] Rossi[11] and Horta,[12] to find elasticity module of carbon Nanotubes, including their chirality. Nevertheless, scarce works are dedicated to analyze the mechanical behavior of a polymer matrix with nanotubes. One of the situations to solve here is how to define the potentials for all components (primary and secondary bonds). Accordingly, the present work proposes a novel solution of such composites, including a non-lineal model of potential bonds, focusing the study on

*Author to whom correspondence should be addressed.

the free volume behavior, as well as on the Poisson ratio of the composite, as the nanotubes content is varying.

2. THEORETICAL BACKGROUND

Particles (or segments) tend to move during each load cycle and get to a new position. After this movement, the particles could have new neighbors. Based on Newton's Law, the governing equations generalized for all three coordinates are:[13]

$$X_j^i(t+\Delta t) = X_j^i(t) + \lambda(t) * [X_j^i(t) - X_j^i(t-\Delta t)] + F_j^i x(t) * (\Delta t)^2 \quad (1)$$

here, $X_j^i(t)$ (as well as $Y_j^i(t)$, $Z_j^i(t)$) are thee coordinates of the jth segment in the ith chain, $\lambda(t)$ is a kinetic coefficient, and $F_j^i x(t)$ (and also $F_j^i y(t)$, $F_j^i z(t)$) are the forces acting on the segment along each axis. The General force $F(t)$ involves both internal and external forces on each particle. The corresponding Force equation involves the derivative of the potential $U_e(t)$. External forces in this tension case are associated only on boundary particles.

$$F_{ij}(t) = (-\partial U_e(t)/\partial X_{ij}) + F_{ij}^{ext} \quad (2)$$

The analysis is focused on the evaluation of Poisson ratio and Free Volume on the elastic behavior before yielding of the composite. The mechanical model governing this behavior involves the energy deformation as well as nodal load vector, as:[14]

$$\rho \int_{\text{vol}} [N]^T [N] dv \{\ddot{u}\} + \int_{\text{vol}} [B]^T [D][B] dv \{u\} = \begin{Bmatrix} F_x(t) \\ F_y(t) \\ F_z(t) \end{Bmatrix} \quad (3)$$

where $\{u\}$: Nodal displacements vector, $\{\ddot{u}\}$: Nodal acceleration vector, $[N]$: Matrix of shape functions, $[B]$: Matrix of derivatives of shape functions, $[D]$: Matrix of elastic parameters, $(F_x(t), F_y(t), F_z(t))^T$: Nodal load vector, ρ: density.

The interaction between particles and nanotubes is well described by finite elements having the same stiffness properties of a real bond. As described before, the bond stiffness has been obtained from the derivatives of potentials. These forces have a strong nonlinear behavior. The bond stiffnesses are very different on tension and compression. Thus, to solve this case, it is necessary to involve a nonlinear analysis: the stiffness matrix K and the restoring Force F^{nr} will vary with the applied load. The procedure used to solve such a problem in general requires multiple iterations.

Amorphous polymer chains are represented by statistical segments, as proposed originally by Flory,[15] in which several repeating units of a chain are treated as single statistical segment. This model is often called a Coarse Grain Model and allows for simulation at a large scale.

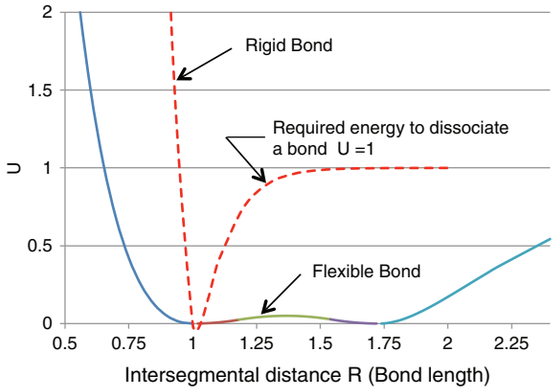

Fig. 1. Potential Energy. Bonding interaction between adjacent segments along a chain.

In this case particles are repeated units of a chain. Specific potentials correspond to different type of bonds, namely:

- Primary (intra-chain) bonds between rigid LC segments.
- Primary (intra-chain) bonds flexible LC segments.
- Secondary bond between particles on neighboring chains.
- Interactions between unlike segments will be treated as rigid, according to Ref. [16].

Primary (intra-chain) bonds between rigid LC segments are described by a steep Morse-like potential limiting the bond extension and their mobility.

$$U_r(R) = [1 - e^{\gamma_r(1-R)}]^2 \quad (4)$$

Primary (intra-chain) bonds flexible LC segments are described by spliced double-well potentials:

$$\begin{cases} [1 - e^{\gamma_f(1-R)}]^2 \\ \quad R \le 1 \\ 8U_0[(1-R)/\Delta]^2 \\ \quad 1 < R \le 1 + 0.25\Delta \\ U_f(R) = U_0\{1 - 8[(1 + 0.5\Delta - R)/\Delta]^2\} \\ \quad 1 + 0.25\Delta < R \le 1 + 0.75\Delta \\ 8U_0[(1 + \Delta - R)/\Delta]^2 \\ \quad 1 + 0.75\Delta < R \le 1 + \Delta \\ [1 - e^{\gamma_f(1+\Delta-R)}]^2 \\ \quad R > 1 + \Delta \end{cases} \quad (5)$$

Here, $\gamma_r = 10$; $\gamma_f = 2$; $U_0 = 0.05$; $\Delta = 0.732$ Units parameters are: $(\text{length})^{-1}$; $(\text{length})^{-1}$; energy and length respectively (see Fig. 1).

3. INTRACHAIN FORCES

The total force on a given particle is the sum of the forces resulting from pairwise interactions and any

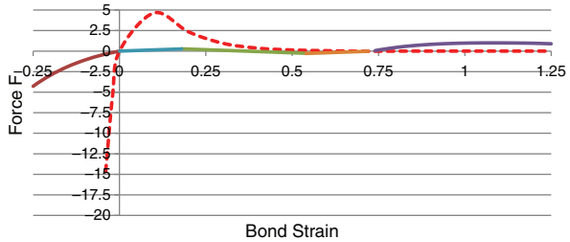

Fig. 2. Force behavior on bonds (F vs. R) for rigid (dashed line) and flexible (full line) cases.

forces applied[17]

$$F_{ij}(t) = (-\partial U_e(t)/\partial R_{ij}) + F_{ij}^{ext} \tag{6}$$

Here, F_{ij} is the force acting on ith segment of the jth chain at time t. U_e is the total configurational energy of the system (sum of pairwise interactions). R_{ij} is the current location of the segment in question, and F_{ij}^{ext} is the external force imposed. So, for a one chain exclusively:

$$F_i(t) = (-\partial U_e(t)/\partial R_i) + F_i^{ext} \tag{7}$$

And for a only one segment of this chain without external forces: $F(t) = -\partial U_e(t)/\partial R$.

So, internal forces on a segment are expressed as derivatives of potentials (Fig. 2).

Secondary bonds occur in rigid and flexible statistical segments (attraction or repulsion forces on particles not belonging to the same chain). Repulsive interaction is generally related to the problem of excluded volume effect and, because of this interaction, there is a resistance to the relative motion of particles between two neighboring chains. These forces are known as van der Walls forces and are different of those related to the bonds between molecules.

Potentials depend on the relative displacements r between neighboring chains.

$$U_e(r) = \begin{cases} 0 \quad r < -\delta \\ 2.5U_0(r/\delta)[0.5(r/\delta)+1]+\lambda \\ \quad -\delta \le r < -0.2\delta \\ U_0[1-5(r/\delta)^2] \\ \quad -0.2\delta \le r \le 0.2\delta \\ 2.5U_0(r/\delta)[0.5(r/\delta)-1]+\lambda \\ \quad 0.2\delta < r \le \delta \\ 0 \quad r > \delta \end{cases} \tag{8}$$

Here, $\delta = 0.5$; $U_0 = 0.05$ for flexible case, and 1.0 for rigid case. Here λ is an adjustable parameter proposed by the present authors. $\lambda = 1.25$ for flexible case, and 0.0625 for rigid case. Units of the parameters are length and energy, respectively. Figure 3, shows the potential Energy

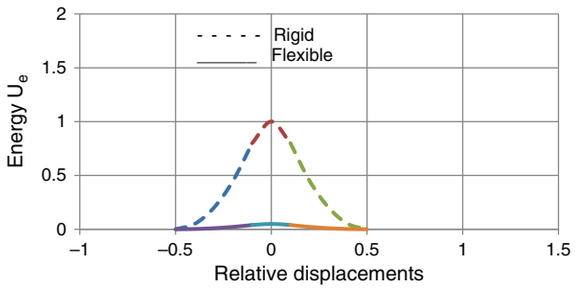

Fig. 3. Energy U_e, versus relative displacement r. Repulsive interaction between neighboring particles on different chains

for both cases. The corresponding interchain forces are shown in Figure 4.

Figure 5 contains a schematic description of each type of bond, according to the elements inside the polymer composite.

Particles (or segments) tend to move during each load cycle and get to a new position. After this movement particles could have new neighbors. According to the literature[16] and based on Newton's Second Law, the governing equations are as follows:

$$\begin{aligned} X_j^i(t+\Delta t) &= X_j^i(t) + \lambda(t) * [X_j^i(t) - X_j^i(t-\Delta t)] \\ &\quad + F_j^i x(t) * (\Delta t)^2 \\ Y_j^i(t+\Delta t) &= Y_j^i(t) + \lambda(t) * [Y_j^i(t) - Y_j^i(t-\Delta t)] \\ &\quad + F_j^i y(t) * (\Delta t)^2 \\ Z_j^i(t+\Delta t) &= Z_j^i(t) + \lambda(t) * [Z_j^i(t) - Z_j^i(t-\Delta t)] \\ &\quad + F_j^i z(t) * (\Delta t)^2 \end{aligned} \tag{9}$$

where, $X_j^i(t)$, $Y_j^i(t)$, $Z_j^i(t)$ are thee coordinates of the jth segment in the ith chain, $\lambda(t)$ is a kinetic coefficient described below, and $F_j^i x(t)$, $Fjiy(t)$, $Fjiz(t)$ are the forces acting on the segment along each axis. Parameter $\lambda(t) = 1$ in case no thermal forces are considered.

The general Force $F(t)$ involves Internal and external forces on each particle. The corresponding Force equation involves the derivative of Potential $U_e(t)$. External

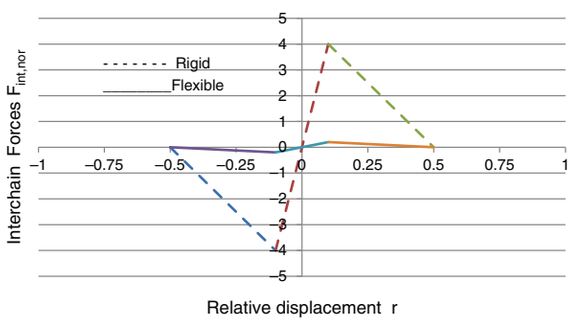

Fig. 4. Interchain Force versus relative displacement r. Interaction between neighboring particles on different chains.

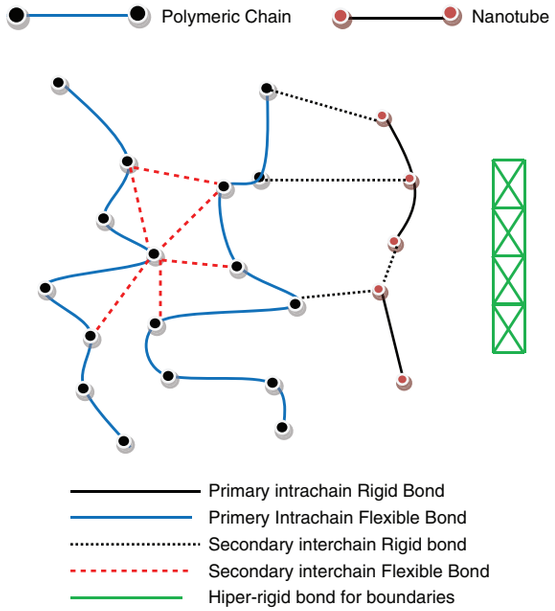

Fig. 5. General Scheme of applied bonds.

Forces in this tension case is associated only to boundary particles.

$$F_{ij}(t) = (-\partial U_e(t)/\partial X_{ij}) + F_{ij}^{ext}$$

Since our analysis is focused on the evaluation of Poisson ratio and Free Volume on elastic behavior before yielding of the composite material, the mechanical model governing this behavior must involve the energy deformation as well as nodal load vector.[18] Matrix discrete model is as follows:

$$\rho \int_{\text{vol}} [N]^T [N] dv\{\ddot{u}\} + \int_{\text{vol}} [B]^T [D][B] dv\{u\} = \begin{Bmatrix} F_x(t) \\ F_y(t) \\ F_z(t) \end{Bmatrix} \tag{10}$$

where: $\{u\}$: Nodal displacements vector, $\{\ddot{u}\}$: Nodal acceleration vector, $[N]$: Matrix of shape functions, $[B]$: Matrix of derivatives of shape functions, $[D]$: Matrix of elastic parameters, $(F_x(t),\ F_y(t),\ F_z(t))^T$: Nodal load vector, ρ: density.

Interaction between particles and Nanotubes is well described by finite elements having the same stiffness properties of a real bond. As described before, the bond stiffness has been calculated from the derivatives of potentials. These forces have a strong nonlinear behavior. The bond stiffness are very different on tension and compression.

Therefore, to solve this case, it is necessary to involve a nonlinear analysis, the stiffness matrix K and the restoring Force F^{nr} will vary with the applied load. The procedure used to solve such a problem in general requires multiple iterations, where each iteration passes through the equation solver.

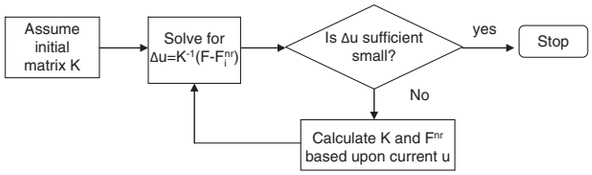

Fig. 6. Non-linear procedure applied for solving dynamic model.

The Finite Element employed in our calculations is a non lineal element named combin39 in ANSYS nomenclature (see Fig. 6). This element is a unidirectional element with nonlinear generalized force-deflection capability. According to,[19] multiwalled carbon nanotubes (MWCN) composed by 8–30 graphene layers have different diameters, between 26 to 76 nanometers, meanwhile, for a single walled carbon nanotube (SWCN) its diameter is of the order 1–4 nm. The length of nanotubes is also variable. By considering an aspect ratio of 13, the corresponding lengths oscillate between 200–1000 nm for MWCN, and 10–50 for SWCN.

Dimensions for Nanotubes adopted in our analysis refers to a multiwall type with 70 nm diameter (0.07 μm), and a length of 500–1500 nm (0.5–1.5 μm) depending of the analyzed case. According to statistical segments dimensions, each segment involves a number of polymer chains, from this point of view proposed by Flori, it is appropriated to take a few segments or a lot segments, it is clear that some behavior of segments will be more clear to follow taking many segments for instance in case of segments entanglements. The diameter of particles we will take analogous to Nanotubes diameter, 0.07 μm.

On a polymer chain, every molecule links with her neighbor through covalent bond and the gap between them is minimum also; segments link one to another through an intrachain bond. In our case, the distance between particles centers is 0.08 μm, with a gap between particles equal to 0.01 μm.

The analysis we will carried out on a sample of dimensions 1.6 μm $\times$ 1.6 μm. Gap-z direction we take as a half of the bond length. Thickness of the sample depends on the number of layers required. The analysis uses 5 layers, so, thickness of the sample will be equal to 0.16 μm. Number of grid points, to place particles and nanotubes inside the sample, would be approximately $(((1.6/0.08)+1)\text{^}2)*4 = 1600$.

The thickness adopted here is one tenth of the sample length. This thickness is thicker than polymer plate samples used on experimental procedures for determining the stress-strain behavior. On the other hand, the number of statistical segments inside of these 1600 points grid seems a good representation of a real composite material. The Elastic module E for a MWCN is about 1.28 TPa. (six time higher than steel). Meanwhile, for a single nanotube

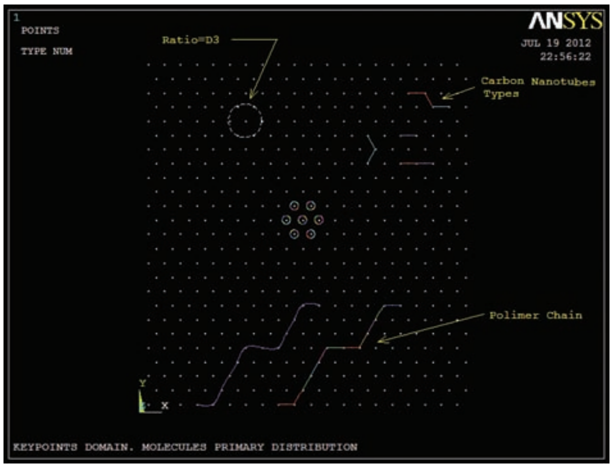

Fig. 7. Different types of Nanotubes inside grid points domain.

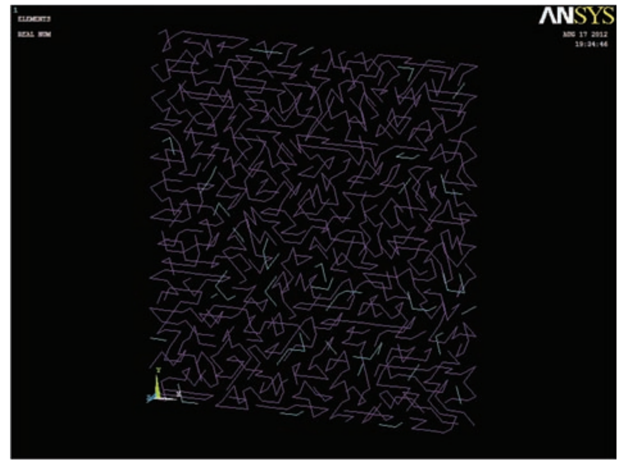

Fig. 9. Polymeric particles and segments (violet). Nanotubes (blue). Percent of Nanotubes in terms of volume of the sample: 5.17%.

module E reach a value of 0.8 TPa. These values show some variation depending of carbon nanotube type (armchair, chiral, etc.) as well as number of walled in case MWCN.

4. RESULTS AND DISCUSSION

Chains construction run smoothly in the computer but, as the process continue, it becomes more and more difficult to built complete chains. The last chains generally are short, even composed by only one or two segments. Thus the procedure adopted for constructing the nanotubes consists on the use of these little chains and adapting them as nanotubes. This procedure has the goal to reduce the amount of little chains used for segments and also for introducing some geometric characteristics on nanotubes as can be the irregular shapes. Figure 7 shows some particularities of this procedure. Parameter $D3 = 0.08$.

The analysis of the composite has been focused on the 3D case (Fig. 8). General dimensions of the composite sample are arbitrary. The parameter "LAY" corresponds to the number of desired layers of the sample, in this case, 5 layers. Gap between layers is of dimension $D3/2$. Gap x of grid points is of dimension $D3$. Gap y of grid points is of dimension $D3 * SQRT(3)$. The second window requires data corresponding to real values of energy, area, and diameters. We have mentioned that our analysis is qualitative, for this reason, all these value area equal to the unity, with the exception for the diameters that are close to the real value for nanotubes and particles.

Evaluation of the main total stress σ_t on the sample was done according to the relationship:

$$\sigma_t = F_t/A_m \tag{11}$$

where:

F_t = Total force on sample = F_n*N_e
F_n = Applied force on each edge node
N_e = Total number of edge nodes
A_m = Sectional area of the sample = $L * t$
t = Thickness of the sample

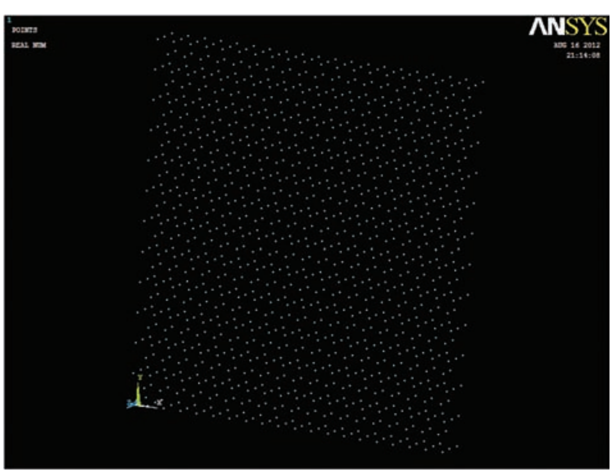

Fig. 8. Isometric view of the layer of points. 3D case.

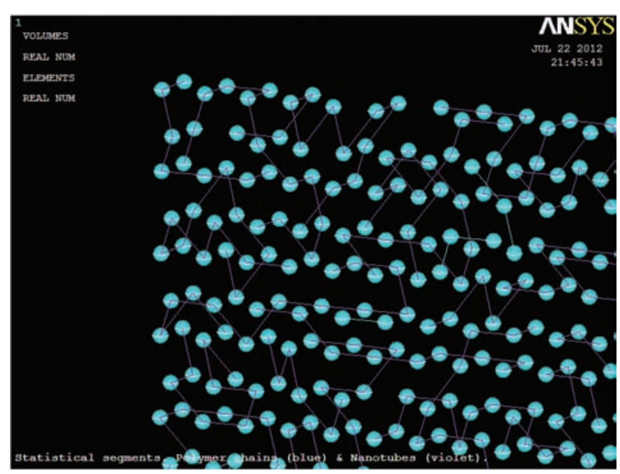

Fig. 10. Close-up of 3D representation of nanotubes and particles.

RESEARCH ARTICLE

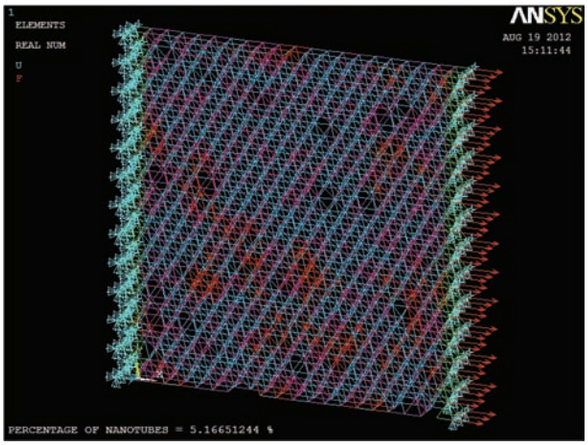

Fig. 11. All Interaction bonds inside model including boundary conditions.

So, total deformation of the sample ε_t:

$$\varepsilon_t = \left(\left(\sum \Delta_{x,n}\right)/N_e\right)/L \tag{12}$$

$\Delta_{x,n} = x$ displacement of an edge node of the sample.

Figures 9 and 10 show the Nanotubes and polymer chains set-up.

Figure 11 shows the obtained set-up of all interaction bonds, together with polymer chains and nanotubes.

Next step was to run the nonlinear analysis. The large displacements procedure was activated. Substeps proposed are: 400, 600, 160. The load was taken as ramped with load increases of 0.005 units. Final applied load was close to 0.08 units. Figure 12 shows the Engineering Stress–Strain behavior, while Figure 13 corresponds to the Real Stress–Strain behavior.

The free volumen V_f of the composite was calculated according to the following relationship:[16]

$$V_f = V_s - (rxV_s + V_n) \tag{13}$$

where V_s is the volume of the composite; r is the number of segments inside the sample; V_s is the volume of individual segment, and V_n is the volume of all nanotubes inside of the sample.

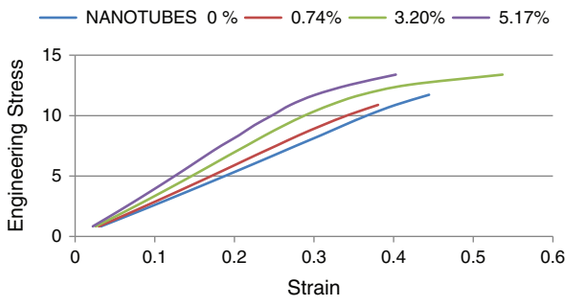

Fig. 12. Engineering Stress-Strain behavior.

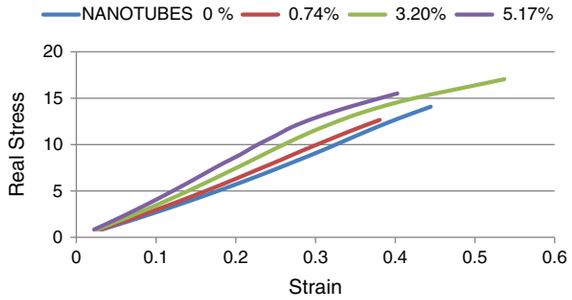

Fig. 13. Real Stress–Strain behavior.

To evaluate the volume of composite we connect all points of layers 1 and 5 (back and front layers) generating a good number of small volumes: the sum of all these volumes is the total volume of the composite. This is a good procedure for the evaluation of deformed volumes on each stage of the analysis. The initial Free-Volume was 0.424 units.

The evaluation of the deformed volumes has been done by taking nodes on the discrete model, instead of geometrical points, due to requirement of the displacement results. First, we proceed to generate a displacement vector to which add the geometrical points initial values. Each load step generates a different vector displacement. One implication of our random procedure to generate the chains geometrical scheme, is that some keypoints do not have a corresponding node, and are required to build the new deformed shape volume. To solve this situation, we generate the additional nodes to cover all the required points domain. This procedure has been done and is part of the computer solution.

The Poisson ratio is obtained by applying the relationship:

$$\mu = \varepsilon_T/\varepsilon_L \tag{14}$$

being ε_T and ε_L the transversal and longitudinal deformation, respectively.

The behavior stress-Poisson ratio (Fig. 14) is as expected: when the percent of nanotube increase, the sample becomes more rigid and displacements diminish, including transversal ones. Poisson ratio values range between 0.26 to 0.40, depending on the nanotubes content.

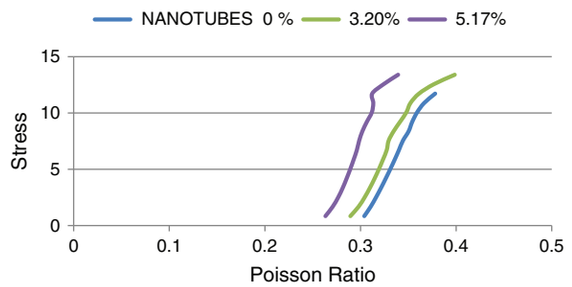

Fig. 14. Stress-Poisson ratio behavior.

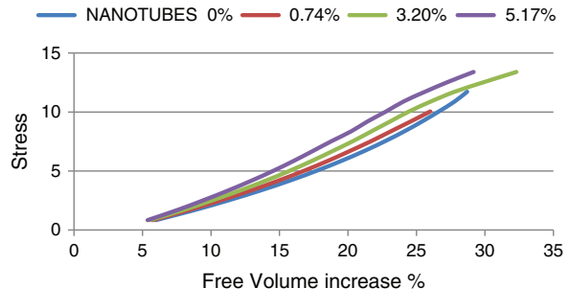

Fig. 15. Stress versus increase on free volume as with respect to the Initial free volume of the sample. Initial volume = 0.424.

The analysis has focused on the elastic behavior prior to yielding of the sample for determining the Poisson ratio variation. On yielding, i.e., when the Poisson ratio is close to 0.5, the material becomes incompressible. Figure 15 corresponds to the change in free volume as a function of the stress.

5. CONCLUSION

The simulations show that, regardless of the amount of segments inside the chains a good mechanical behavior, at least in terms of elasticity, very close to those results obtained by Simoes[16] can be obtained by adding even a small amount of nanotubes. Our results also show that material yield and flow only occurs when an important quantity of secondary bonds fails. Also, the plastic behavior happens when primary bonds are subjected to big strains.

Acknowledgment: This research was done thanks to the support of the National Council of Science and Technology of Mexico (CONACYT) as well as the support of the Laboratory of Advanced Polymers and Optimized Materials (LAPOM) at the University of North Texas, USA.

References

1. P. M. Ajayan, O. Stephan, C. Colliex, and D. Trauth, *Science* 265, 1212 (**1994**).
2. M. M. Treacy, T. W. Ebessen, and J. M. Gibson, *Nature* 381, 678 (**1996**).
3. S. Kanagaraj, F. R. Varanda, T. V. Zhil'tsova, M. S. A. Oliveira, and J. A. O. Simoes, *Compos. Sci. Technol.* 67, 3071 (**2007**).
4. Z. Wang, P. Ciselli, and T. Peijs, *Nanotechnology* 18, 455709/1 (**2007**).
5. Q. Zeng, A. Yu, and G. Lu, *Prog. Polym. Sci.* 33, 191 (**2008**).
6. A. Nakano, M. Bachlechner, R. Kalia, E. Lidorikis, P. Vashishta, G. Voyiadjis, T. Campbell, S. Ogata, and F. Shimojo, *Comput. Sci. Eng.* 3, 56 (**2001**).
7. A. Uhlherr and D. Theodorou, *Solid State and Materials Science* 3, 544 (**1998**).
8. A. Guillaume and M. Jean-Francois, *9e Colloque National en Calcul des Structures* 1, 233 (**2009**).
9. W. Wang, An Adaptive Multi-Scale Computational Method for Modeling Nonlinear Deformation in Nanoscale Materials, Dissertation Submitted to the Graduate Faculty of the Louisiana University, Baton Rouge, Louisiana (**2006**).
10. T. Belytschko, *Phys. Rev. B.* 65, 235430 (**2002**).
11. M. Rossi and M. Meo, *Compos. Sci. Technol.* 69, 1394 (**2009**).
12. R. J. Horta, W. Brostow, and V. Castaño, *Polimery* 58, 276 (**2013**).
13. R. Simoes, A. M. Cunha, and W. Brostow, *Comp. Mater. Sci.* 36, 319 (**2006**).
14. R. D. Cook, D. S. Malkus, and M. E. Plesha, Concepts and Applications of Finite Element Analysis, John Wiley and Sons, Inc., New York (**1988**).
15. P. J. Flory and M. Volkenstein, Statistical Mechanics of Chain Molecules, John Wiley and Sons, Inc. New York (**1969**).
16. R. Simoes, A. M. Cunha, and W. Brostow, *Modelling Simul. Mater. Sci. Eng.* 14, 157 (**2006**).
17. S. Blonski and W. Brostow, *J. Chem. Phis.* 95, 2890 (**1991**).
18. Manual ANSYS, Inc., Software, Canonsburgh PA, USA (**2009**), Ver. 11.
19. J. P. Salvetat, J. M. Bonard, N. H. Thomson, A. J. Kulik, L. Forr'o, W. Benoit, and L. Zuppiroli, *Appl. Phys. A.* 69, 255 (**1999**).

Received: 6 September 2014. Accepted: 27 September 2014.